Distributed measurement of dynamic strain based on multi-slope assisted fast BOTDA

Dexin Ba,[1,2] Benzhang Wang,[1] Dengwang Zhou,[1] Mingjing Yin,[3] Yongkang Dong,[1,*] Hui Li,[4] Zhiwei Lu,[1] and Zhigang Fan[5]

[1]*National Key Laboratory of Science and Technology on Tunable Laser, Harbin Institute of Technology, Harbin 150001, China*
[2]*Faculty of Engineering, Bar-Ilan University, Ramat-Gan 52900, Israel*
[3]*Harbin Medical University, Harbin 150081, China*
[4]*School of Civil Engineering, Harbin Institute of Technology, Harbin 150001, China*
[5]*Research Center for Space Optical Engineering, Harbin Institute of Technology, Harbin 150001, China*
[*]*aldendong@gmail.com*

Abstract: We propose and demonstrate a dynamic Brillouin optical fiber sensing based on the multi-slope assisted fast Brillouin optical time-domain analysis (F-BOTDA), which enables the measurement of a large strain with real-time data processing. The multi-slope assisted F-BOTDA is realized based on the double-slope demodulation and frequency-agile modulation, which significantly increases the measurement range compared with the single- or double- slope assisted F-BOTDA, while maintaining the advantage of fast data processing and being suitable for real-time on-line monitoring. A maximum strain variation up to 5000με is measured in a 32-m fiber with a spatial resolution of ~1m and a sampling rate of 1kHz. The frequency of the strain is 12.8Hz, which is limited by the rotation rate of the motor used to load the force on the fiber. Furthermore, the influence of the frequency difference between two adjacent probe tones on the measurement error is studied theoretically and experimentally for optimization. For a Brillouin gain spectrum with a 78-MHz width, the optimum frequency difference is ~40MHz. The measurement error of Brillouin frequency shift is less than 3MHz over the whole measurement range (241MHz).

OCIS codes: (060.2370) Fiber optics sensors; (290.5830) Scattering, Brillouin; (190.0190) Nonlinear optics.

References and links

1. T. Kurashima, T. Horiguchi, and M. Tateda, "Distributed-temperature sensing using stimulated Brillouin scattering in optical silica fibers," Opt. Lett. **15**(18), 1038–1040 (1990).
2. M. A. Soto, G. Bolognini, and F. Di Pasquale, "Long-range simplex-coded BOTDA sensor over 120 km distance employing optical preamplification," Opt. Lett. **36**(2), 232–234 (2011).
3. Y. Dong, L. Chen, and X. Bao, "Extending the sensing range of Brillouin optical time-domain analysis combining frequency-division multiplexing and in-line EDFAs," J. Lightwave Technol. **30**(8), 1161–1167 (2012).
4. X. Bao and L. Chen, "High performance BOTDA for long range sensing," Proc. SPIE **7982**, 798206 (2011).
5. M. A. Soto, X. Angulo-Vinuesa, S. Martin-Lopez, S.-H. Chin, J. D. Ania-Castanon, P. Corredera, E. Rochat, M. Gonzalez-Herraez, and L. Thévenaz, "Extending the real remoteness of long-range Brillouin optical time-domain fiber analyzers," J. Lightwave Technol. **32**(1), 152–162 (2014).
6. J. Urricelqui, M. Sagues, and A. Loayssa, "Synthesis of Brillouin frequency shift profiles to compensate non-local effects and Brillouin induced noise in BOTDA sensors," Opt. Express **22**(15), 18195–18202 (2014).
7. K. Hotate and M. Tanaka, "Distributed fiber Brillouin strain sensing with 1-cm spatial resolution by correlation-based continuous-wave technique," IEEE Photonics Technol. Lett. **4**(2), 179–181 (2002).
8. K. Song, Z. He, and K. Hotate, "Distributed strain measurement with millimeter-order spatial resolution based on Brillouin optical correlation domain analysis and beat lock-in detection scheme," in *Optical Fiber Sensors*, OSA Technical Digest (CD) (Optical Society of America, 2006), paper ThC2.
9. Y. Dong, H. Zhang, L. Chen, and X. Bao, "2 cm spatial-resolution and 2 km range Brillouin optical fiber sensor using a transient differential pulse pair," Appl. Opt. **51**(9), 1229–1235 (2012).

#258384 Received 2 Feb 2016; revised 22 Apr 2016; accepted 23 Apr 2016; published 27 Apr 2016

10. Y. London, Y. Antman, R. Cohen, N. Kimelfeld, N. Levanon, and A. Zadok, "High-resolution long-range distributed Brillouin analysis using dual-layer phase and amplitude coding," Opt. Express **22**(22), 27144–27158 (2014).
11. A. Minardo, A. Coscetta, L. Zeni, and R. Bernini, "High-spatial resolution DPP-BOTDA by real-time balanced detection," IEEE Photonics Technol. Lett. **26**(12), 1251–1254 (2014).
12. L. Thévenaz, A. Denisov, and M. A. Soto, "Brillouin distributed fiber sensing at ultra-high spatial resolution," in *Photonics Conference* (IPC, 2015), pp. 337–338.
13. D. Culverhouse, F. Farahi, C. N. Pannell, and D. A. Jackson, "Potential of stimulated Brillouin scattering as sensing mechanism for distributed temperature sensors," Electron. Lett. **25**(14), 913–915 (1989).
14. T. Horiguchi, T. Kurashima, and M. Tateda, "Tensile strain dependence of Brillouin frequency shift in silica optical fibers," IEEE Photonics Technol. Lett. **1**(5), 107–108 (1989).
15. K. Y. Song and K. Hotate, "Distributed fiber strain sensor with 1 kHz sampling rate based on Brillouin optical correlation domain analysis," Proc. SPIE **6770**, 67700J (2007).
16. Y. Mizuno, Z. He, and K. Hotate, "One-end-access high-speed distributed strain measurement with 13-mm spatial resolution based on Brillouin optical correlation-domain reflectometry," IEEE Photonics Technol. Lett. **21**(7), 474–476 (2009).
17. R. Bernini, A. Minardo, and L. Zeni, "Dynamic strain measurement in optical fibers by stimulated Brillouin scattering," Opt. Lett. **34**(17), 2613–2615 (2009).
18. Y. Peled, A. Motil, and M. Tur, "Fast Brillouin optical time domain analysis for dynamic sensing," Opt. Express **20**(8), 8584–8591 (2012).
19. J. Urricelqui, A. Zornoza, M. Sagues, and A. Loayssa, "Dynamic BOTDA measurements based on Brillouin phase-shift and RF demodulation," Opt. Express **20**(24), 26942–26949 (2012).
20. A. Voskoboinik, A. E. Willner, and M. Tur, "Extending the dynamic range of sweep-free Brillouin optical time-domain analyzer," J. Lightwave Technol. **33**(14), 2978–2985 (2015).
21. K. Y. Song, M. Kishi, Z. He, and K. Hotate, "High-repetition-rate distributed Brillouin sensor based on optical correlation-domain analysis with differential frequency modulation," Opt. Lett. **36**(11), 2062–2064 (2011).
22. Y. Dong, D. Ba, T. Jiang, D. Zhou, H. Zhang, C. Zhu, Z. Lu, H. Li, L. Chen, and X. Bao, "High-spatial-resolution fast BOTDA for dynamic strain measurement based on differential double-pulse and second-order sideband of modulation," IEEE Photonics J. **5**(3), 2600407 (2013).
23. I. Sovran, A. Motil, and M. Tur, "Frequency-scanning BOTDA with ultimately fast acquisition speed," IEEE Photonics Technol. Lett. **27**(13), 1426–1429 (2015).
24. Y. Peled, A. Motil, L. Yaron, and M. Tur, "Slope-assisted fast distributed sensing in optical fibers with arbitrary Brillouin profile," Opt. Express **19**(21), 19845–19854 (2011).
25. A. Motil, O. Danon, Y. Peled, and M. Tur, "Pump-power-independent double slope-assisted distributed and fast Brillouin fiber-optic sensor," IEEE Photonics Technol. Lett. **26**(8), 797–800 (2014).
26. A. Minardo, A. Coscetta, R. Bernini, and L. Zeni, "Heterodyne slope-assisted Brillouin optical time-domain analysis for dynamic strain measurements," J. Opt. **18**(2), 025606 (2016).
27. A. Motil, R. Hadar, I. Sovran, and M. Tur, "Gain dependence of the linewidth of Brillouin amplification in optical fibers," Opt. Express **22**(22), 27535–27541 (2014).

1. Introduction

Brillouin optical fiber sensing has attracted great interest since 1990s [1]. Excellent researches have been carried out to extend the sensing range [2–6] and improve the spatial resolution [7–12]. It is based on the simple and linear relationship between the Brillouin frequency shift (BFS) and strain (temperature) [13,14]. Generally, Brillouin analysis techniques use the scanning of the Brillouin gain spectrum (BGS) and curve fitting to realize the measurement of BFS. Because of the relative low frequency-tuning speed, traditional Brillouin analysis mainly focuses on the measurement of static or slowly-varied signal. In order to realize the sensing for rapidly changed signals (especially for the dynamic strains deriving from vibration), several techniques have been proposed in recent years [15–20]. By employing a Brillouin optical correlation domain analysis (BOCDA) technique, a 200-Hz strain was measured in a segment of 20-m fiber [15]. Because the BOCDA system utilizes correlation peaks for the measurement, a scanning of the location of the peaks is essential for the distributed measurement along the whole fiber, which decreases its sampling rate for a long sensing fiber [21]. Peled and coauthors proposed a frequency-agile method based on a pre-programming of arbitrary wave generators (AWG) to realize fast BOTDA (F-BOTDA), where a 100-Hz strain was measured with 1-m spatial resolution over a 100-m fiber [18]. A high-spatial-resolution F-BOTDA based on differential double-pulse and second-order sideband modulation was proposed by our group, where a measurement of 50-Hz vibration with the spatial resolution of 20cm in a 50-m polarization maintaining (PM) fiber was realized [22]. Further, a polarization-

#258384 Received 2 Feb 2016; revised 22 Apr 2016; accepted 23 Apr 2016; published 27 Apr 2016

independent F-BOTDA was proposed to eliminate the polarization fading existed in the standard single mode fiber (SMF), where two orthogonal pulsed pumps together with two co-polarized probes were employed. The ultimate measurement speed of 9700 [full-BGS]/second was demonstrated in a 145-m standard SMF, covering a strain dynamic range of 4200με [23]. The BFS is demodulated via curve fitting in the frequency-scanning methods above. It is time-consuming and generally takes much more time than data acquisition, especially for the long range sensing, which makes them not suitable for the real-time on-line monitoring, even though high efficient compiled programing techniques (such as C and Cpp) are employed in curve fitting algorithms. Alternatively, slope-assisted measurements follow changes of the BFS by monitoring the gain of a single probe tone that is slightly detuned from the gain peak [17,24], which is an excellent candidate for real-time on-line sensing. What's more, a modified slope-assisted method—double slope-assisted method was proposed, which was successful to suppress the pump power variation induced error and a strain variation up to ~160με was measured with the sampling rate of 1kHz [25]. Recently, another pump-power independent slope-assisted method was proposed, where the probe was phase-modulated and the gains of the first-order sidebands and the carrier were used to eliminate the influence of pump power variation. In experiment, a 150-με strain was measured, the frequency of which was 1.8Hz [26]. However, the measurement ranges of these slope-assisted methods are restricted by the scale of the slope (generally less than 1000με [17]).

In this paper, we propose a dynamic distributed Brillouin sensing based on multi-slope assisted fast BOTDA, which is capable of extending the measurement scale significantly. This method employs a frequency-agile method to generate a multi-tone probe wave, which forms multiple slopes of BGS in the FUT and extends the measurement range of strain from single slope to several slopes. Meanwhile, because the BFS is demodulated via a linear and non-curve-fitting algorithm, the multi-slope assisted F-BOTDA provides an excellent real-time measurement. Furthermore, the number of the probe tones is reduced in a great amount compared with the curve-fitting method, which makes it possible to measure a more rapidly changed strain. In experiment, a dynamic strain of 5000με of 12.8Hz is measured in a 32-m PM fiber with a spatial resolution of 1m. The influence of the frequency difference between two adjacent probe tones on the measurement error is studied theoretically and experimentally for optimization. For a Brillouin gain spectrum with a 78-MHz width, the optimum frequency difference is ~40MHz. The measurement error of the BFS is less than 3MHz over the whole measurement range (241MHz).

2. Principles

The measurement range, which is limited by the scale of the linear region of the BGS in the single or double slope-assisted analysis, is extended by the construction of the multiple slopes of BGS in the FUT. The sketch map of the multi-slope assisted F-BOTDA is shown in Fig. 1. The left part denotes the double-slope assisted BOTDA, and the right part denotes multi-slope assisted F-BOTDA. In the scheme of the double-slope assisted BOTDA, the spectrum of the probe wave consists of only two tones with the frequency difference of $\Delta\upsilon_{\Gamma}$, which are marked as Tone 1 and Tone 2 in the left part of this figure. The BFS is calculated via the ratio of the gains of the two tones. The measurement scale of the double-slope method is limited by the width of the slope. Nevertheless, if more tones in the probe spectrum are generated, as shown in the right part of Fig. 1, the situation is changed. When the BFS is between Tone 1 and Tone 2, it can be demodulated by the gains of Tone 1 and Tone 2, which uses the same algorithm as the double-slope method. When the BFS is between Tone 2 and Tone 3, these two tones are valid for the calculation of the BFS. So the BFS can be determined via a pair of neighbor tones. Because the frequency differences between the probe tones and the pump are known, the BFS can be demodulated. Considering the influence of the signal noise ratio (SNR), a comparison of the intensities of the tones is carried out to choose two adjacent tones with relative higher intensities for the demodulation of the BFS.

#258384 Received 2 Feb 2016; revised 22 Apr 2016; accepted 23 Apr 2016; published 27 Apr 2016

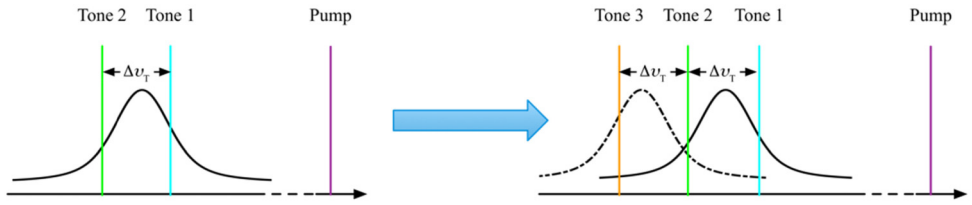

Fig. 1. Basic idea of the extension of measurement range by multi-slope assisted F-BOTDA.

The sketch map of the interaction of pump pulses and the probe wave is shown in Fig. 2, where pump pulses meet a probe sequence consisting of several tones in the FUT. The time interval between two neighbor pump pulses is ΔT , which is determined by the length of the FUT in order to satisfy that one probe tone interacts with only one pump pulse. These probe tones, with the frequency difference of $\Delta\upsilon_T$ which is much larger than the scanning step in curve-fitting based F-BOTDA [22], are successively injected into the FUT.

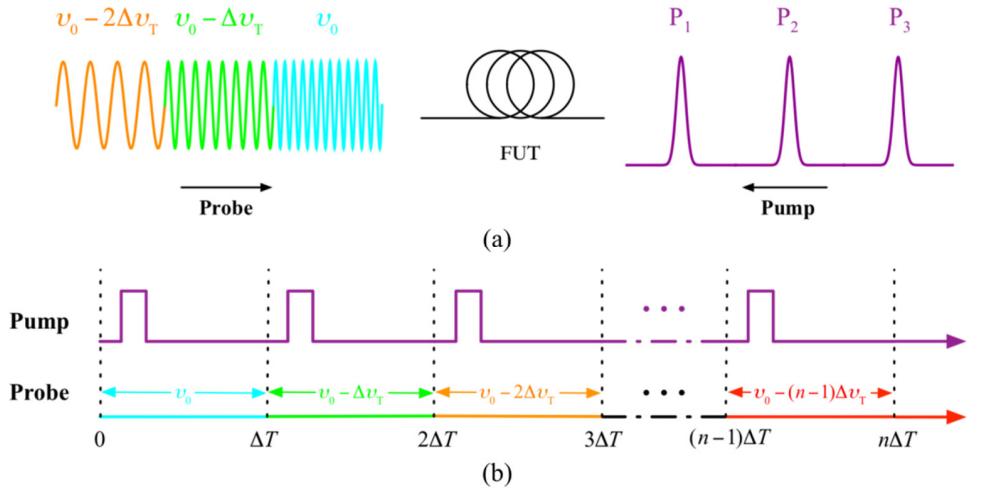

Fig. 2. (a) Sketch map of multi-slope assisted F-BOTDA; (b) time sequence diagram of the probe and pump.

The generation of the multi-tone probe is the basis for the multi-slope assisted F-BOTDA. Here we utilize a frequency-agile method with the second-order sideband of modulation via an AWG [22]. For achieving the multi-tone probe mentioned above, the electrical signal generated by the AWG should be composed of a series of sine waves. The frequency of the electrical signal satisfies:

$$f_{\mathrm{AWG}}(t)=f_0+\left[\frac{t}{\Delta T}\right]\frac{\Delta\upsilon_T}{2}. \tag{1}$$

where $[x]$ denotes the integral part of x. By adjusting the DC bias of the electro optic modulator (EOM) and the intensity of RF signal, the second-order sidebands are generated. Then using a fiber Bragg grating, we can get the lower second-order sideband, which works as the probe sequence.

#258384 Received 2 Feb 2016; revised 22 Apr 2016; accepted 23 Apr 2016; published 27 Apr 2016

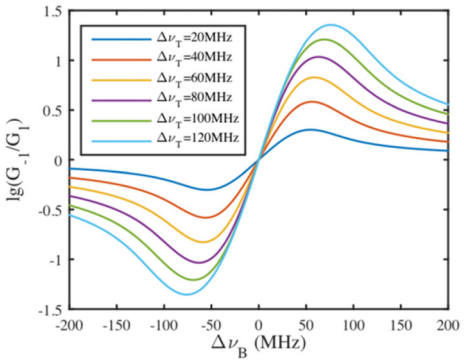

Fig. 3. Relations between the logarithmic ratio of the gain and the variation of the BFS. The FWHM of the BGS is 78MHz, corresponding to the FUT in the experiment below.

The BFS is calculated based on the gains of two adjacent probe tones and the profile of BGS [25]. Supposing the frequencies of two tones satisfy:

$$\begin{aligned} \upsilon_1 &= \upsilon_P - \upsilon_{B0} + 0.5\Delta\upsilon_T \\ \upsilon_{-1} &= \upsilon_P - \upsilon_{B0} - 0.5\Delta\upsilon_T . \end{aligned} \tag{2}$$

Where υ_P is the frequency of the pump and υ_{B0} is the initial value of the BFS. Using the profile of the BGS, the relation between the logarithmic ratio (base 10) of the gains of the two tones and the change of the BFS (denoted as $\Delta\upsilon_B = \upsilon_B - \upsilon_{B0}$) can be obtained, which is shown in Fig. 3, where the full width at half maximum (FWHM) of the BGS is 78MHz, corresponding to the width of the BGS of the FUT in the experiment below. There is a valid region where the values of $\lg(G_{-1}/G_1)$ and $\Delta\upsilon_B$ follow one-to-one relationship, which can be used to calculate $\Delta\upsilon_B$ using $\lg(G_{-1}/G_1)$. For the double-slope assisted F-BOTDA, the width of the valid region limits the measurement range of strain. When it comes to the multi-slope assisted BOTDA, the width of the valid region is more crucial, which determines whether the multi-slope method is capable of extending the measurement range. When the width of the valid region is less than $\Delta\upsilon_T$, the measurement range of strain is not continuous for the multi-slope method, which means the failure to extend the measurement range. The width is calculated for various $\Delta\upsilon_T$ in our analysis. Figure 4 shows the width of the valid region for various $\Delta\upsilon_T$ ranging from 10MHz to 120MHz. A dash line with the slope coefficient of 1 is added in this figure. All the data above the dash line means the width of valid region is larger than $\Delta\upsilon_T$. It is clear that the width of the valid region is larger than $\Delta\upsilon_T$. So the multi-slope assisted F-BOTDA is feasible for $\Delta\upsilon_T$ ranging from 10MHz to 120MHz.

#258384 Received 2 Feb 2016; revised 22 Apr 2016; accepted 23 Apr 2016; published 27 Apr 2016

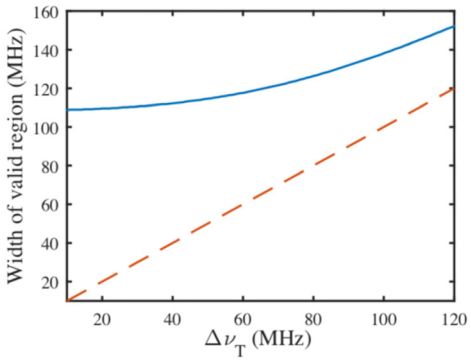

Fig. 4. Width of the valid region for the calculation of the BFS for various $\Delta\upsilon_T$, which is denoted via blue curve. A line with the slope coefficient of 1 is drawn for reference.

The measurement noise of the gains of the probe tones leads to the BFS measurement error, which leads to strain measurement error. It exists in all the slope-assisted F-BOTDA techniques. In order to figure out how significant the error is and how to minimize the influence, the noise induced BFS measurement errors is analyzed. Firstly, the noise is treated as Gaussian noise, where two statistical parameters, i.e., the average value of the deviation of gains and its standard deviation (unbiased estimator) are employed, which are defined as follows:

$$\begin{aligned}\mu_E &= \frac{1}{n}\sum_{i=1}^{n}\left(g_{mi}-g_{ci}\right)\\ \sigma_E &= \sqrt{\frac{1}{n-1}\sum_{i=1}^{n}\left(g_{mi}-g_{ci}-\mu_E\right)^2}.\end{aligned} \tag{3}$$

where g_m and g_c represent the measured and calculated gain respectively. Three pairs of μ_E and σ_E are used for the simulation, i.e., (0.0178, 0.0514), (0.0178 × 0.5, 0.0514 × 0.5) and (0.0178 × 2, 0.0514 × 2), where (0.0178, 0.0514) is the typical value of noise according to our experiment which is described in the next section. The measurement error of the BFS is calculated for various $\Delta\upsilon_T$ ranging from 10MHz to 80MHz. Furthermore, considering that the error may vary with the BFS, the error is calculated for different $\Delta\upsilon_B$, ranging from 0 to 300MHz in order to obtain a comprehensive estimate. For each $\Delta\upsilon_T$, the BFS measurement error is estimated via the averaged absolute value of error and its deviation over the whole range of $\Delta\upsilon_B$, the definitions are as follows:

$$\begin{aligned}\mu_{E\_\upsilon_B} &= \frac{1}{n}\sum_{i=1}^{n}\left|\upsilon_{B\_mi}-\upsilon_{B\_ci}\right|\\ \sigma_{E\_\upsilon_B} &= \sqrt{\frac{1}{n-1}\sum_{i=1}^{n}\left(\left|\upsilon_{B\_mi}-\upsilon_{B\_ci}\right|-\mu_{E\_\upsilon_B}\right)^2}.\end{aligned} \tag{4}$$

where υ_{B_m} and υ_{B_c} represent the actual and calculated BFS respectively. Here n equals 301 because $\Delta\upsilon_B$ is changed from 0 to 300MHz with the step of 1MHz. So each value of $\mu_{E\_\upsilon_B}$ ($\sigma_{E\_\upsilon_B}$) represents the statistic result of the error over the whole range of $\Delta\upsilon_B$ (from 0 to 300MHz). The simulation is carried out for 10 times, the results of which are shown in Fig.

#258384 Received 2 Feb 2016; revised 22 Apr 2016; accepted 23 Apr 2016; published 27 Apr 2016

5. From this figure, we can see that the minimum measured error is obtained when $\Delta\upsilon_T$ is ~40MHz, which is approximately the half of the FWHM of the BGS (78MHz). For a relatively larger $\Delta\upsilon_T$, the measurement error increases, which results from that the data in the tails of the BGS is employed to calculate the BFS, where the SNR is relatively low. While on the other side, too small $\Delta\upsilon_T$ also leads to the increase of error, which is mainly because that $\left|\mathrm{d}\Delta\upsilon_B/\mathrm{d}\left[\lg\left(G_{-1}/G_1\right)\right]\right|$ increases while $\Delta\upsilon_T$ decreases, as shown in Fig. 3.

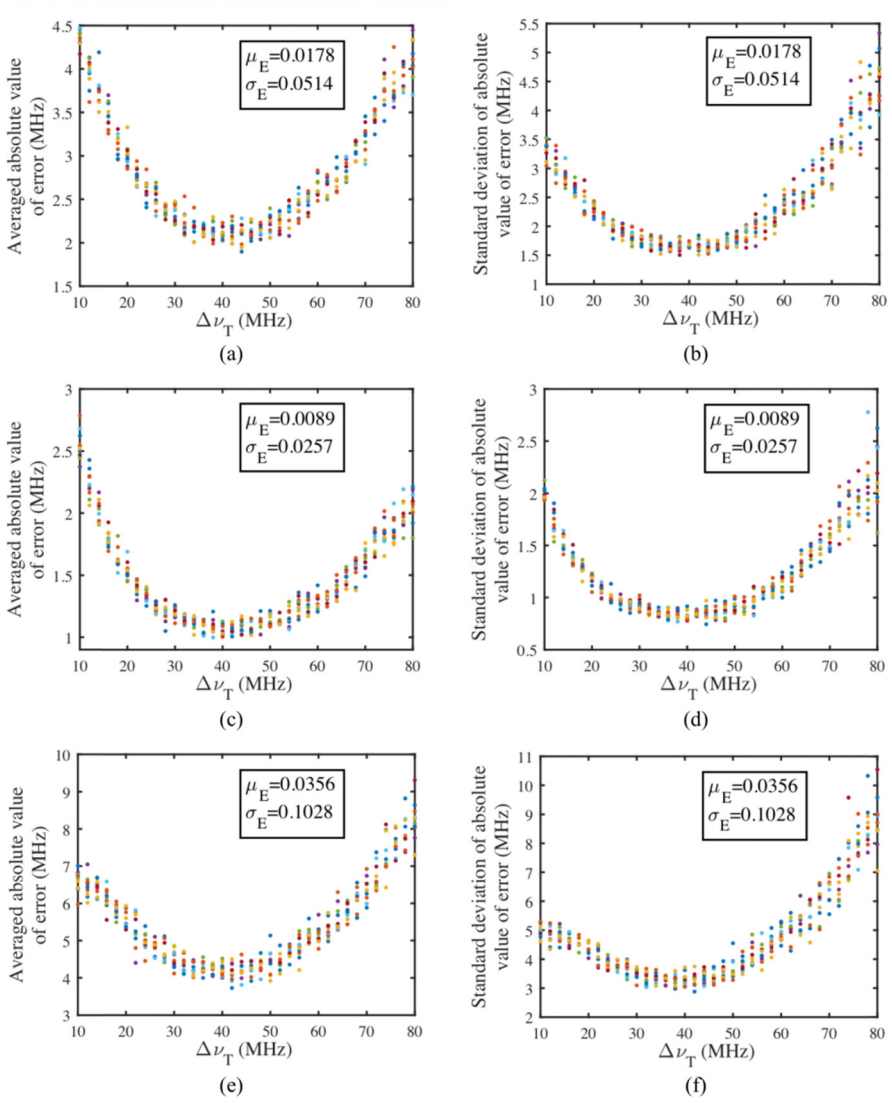

Fig. 5. noise-induced error of the BFS for various $\Delta\upsilon_T$, ranging from 10MHz to 80MHz. μ_E and σ_E are the average value of the deviation of gains and its standard deviation (unbiased estimator) of Gaussian noise. (μ_E = 0.0178, σ_E = 0.0514) corresponds to the experimental results in the next section. The FWHM of the BGS is 78MHz.

#258384 Received 2 Feb 2016; revised 22 Apr 2016; accepted 23 Apr 2016; published 27 Apr 2016

3. Experimental results and discussions

The experimental setup is shown in Fig. 6. The laser source is a distributed feedback optical fiber laser with an ultra-narrow linewidth (40kHz), the output of which is divided by a 3-dB coupler into two parts. One part is modulated by an electro-optic modulator (EOM1) to form 8.4-ns Gaussian pulses, which leads to a broadened BGS. Because the width of the BGS determines the scale of the single slope, a broader BGS means a larger measurement range with one slope. In other words, for a given measurement range, fewer tones or slopes are required and it can also increase the maximum sampling rate. Here we choose Gaussian pulses rather than square pulses to remove the oscillation in the tails of the BGS. The pump pulses are amplified by an erbium doped fiber amplifier (EDFA) and then injected into a 32-m PM fiber, a ~2-m section of which is stretched by an off-axis plate driven by an electrical motor to generate dynamic strains. The other part is modulated by EOM2, which is driven by an AWG. The AWG generates the electrical signal as described in Eq. (1), which is then amplified by an electrical amplifier to modulate the input beam. By adjusting the amplitude of the electrical signal and DC bias to suppress the odd-order bands and carrier, the second-order sidebands are generated. After filtered by an optical filter (FBG), the lower second-order sideband is obtained. Two polarization controllers (PC2 and PC3) are used to adjust the polarization state to ensure both the pump and probe traveling along the same axis of the FUT. The powers of the pump and probe wave are 1W and 68μW respectively. Pump pulses and probe tones are synchronized by the AWG. An oscilloscope is used to record the amplified probe. It is triggered by the AWG with an interval of 1ms. So we can get 1000-frame gains of the probe wave per second. A moving average of order 5 is used to improve the SNR. That is, every 5 frames of gains are averaged.

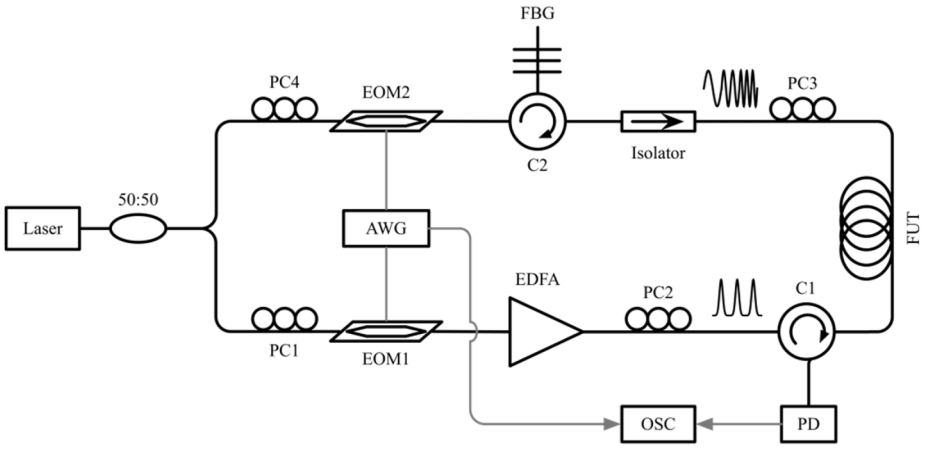

Fig. 6. Experimental setup of distributed dynamic sensing based on multi-slope assisted F-BOTDA (PC: polarization controller, EOM: electro-optic modulator, FBG: fiber Bragg grating, C: circulator, EDFA: erbium doped fiber amplifier, FUT: fiber under test, AWG: arbitrary waveform generator, PD: photodetector, OSC: oscilloscope).

In order to verify the feasibility of measuring strains via multi-slope assisted F-BOTDA and analyze its performance under different parameters, two kinds of demodulation techniques are utilized, i.e., multi-slope assisted F-BOTDA and curve-fitting based F-BOTDA [18], the latter of which is used to examine the performance of the multi-slope method. Although the demodulation algorithms of the BFS in the two methods are completely different, the data used in the multi-slope method is only a part of the data acquired in the curve-fitting method, which makes it possible to carry out the two methods simultaneously and makes the comparison more reliable. In order to measure dynamic strains via the two methods simultaneously, the frequency agile range is from 10870MHz to 11200MHz, with a

#258384 Received 2 Feb 2016; revised 22 Apr 2016; accepted 23 Apr 2016; published 27 Apr 2016

step of 4MHz, which is much smaller than $\Delta\upsilon_{\Gamma}$ used in multi-slope method. The gains of all the probe tones used for the demodulation of the BFS via curve-fitting method, are denoted as a set as $\{G_i\}$, where i = 1,2,3…, is the index of tones. The subset of data used for the demodulation of the BFS via multi-slope method is:

$$\left\{ G_{\frac{\upsilon_{\mathrm{PPm\_0}}-10870+(j-1)\Delta\upsilon}{4}+1} \right\}, j = 1,2,3... \tag{5}$$

where $\upsilon_{\mathrm{PPm\_0}}$ is the frequency difference between pump and the first probe tone in multi-slope method.

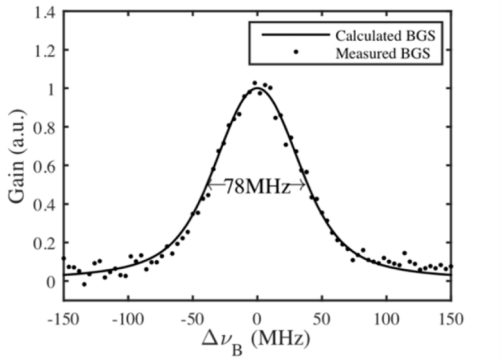

Fig. 7. Measured Brillouin gain spectrum with a FWHM of 78MHz.

Firstly, the BGS is measured via curve-fitting based F-BOTDA, which is shown in Fig. 7. The dots represent the measured data, while the solid line represents the theoretically calculated BGS obtained by the convolution of the pump power spectral density and the intrinsic Brillouin gain curve [14]. As mentioned above, the average value of the error and the standard deviation of error are 0.0178 and 0.0514 respectively. The width of the BGS is used to estimate the number of probe tones needed for the measurement of the stain.

The measured dynamic BFS and strain are shown in Fig. 8, where Figs. 8(a)-8(d) are corresponding to $\Delta\upsilon_{\Gamma}$ = 20MHz, 40MHz, 60MHz and 80MHz respectively, and $\upsilon_{\mathrm{PPm\_0}}$ = 10840MHz, which is less than the BFS in free state (10842MHz), in order to assure that all the BFS can be determined by two neighbor slopes. The variation of the dynamic strains is about 5000με, corresponding to 241-MHz change of the BFS, which is far beyond the limitation of slope-assisted analysis. The frequency of strain is ~12.8Hz, which is limited by the power of the motor. The sold lines denote the measured BFS via multi-slope method, while the dotted curves denote the results obtained via curve-fitting method. Noted that the results of the multi-slope method with $\Delta\upsilon_{\Gamma}$ = 40MHz and 60MHz, as shown in Figs. 8(b) and 8(c), are in better agree with the results obtained via curve-fitting method. A quantitative analysis of measurement error is shown in shown in Fig. 9, the trend of which conforms with Fig. 5. The measured errors are slightly larger than the theoretical analysis, which results from the width change of the BGS [27]. This kind of error source exists in not only the multi-slope analysis, but also in all the other slope assisted Brillouin analysis techniques, including single- and double- slope analysis. Further research would emphasis on how to suppress its influence.

#258384 Received 2 Feb 2016; revised 22 Apr 2016; accepted 23 Apr 2016; published 27 Apr 2016

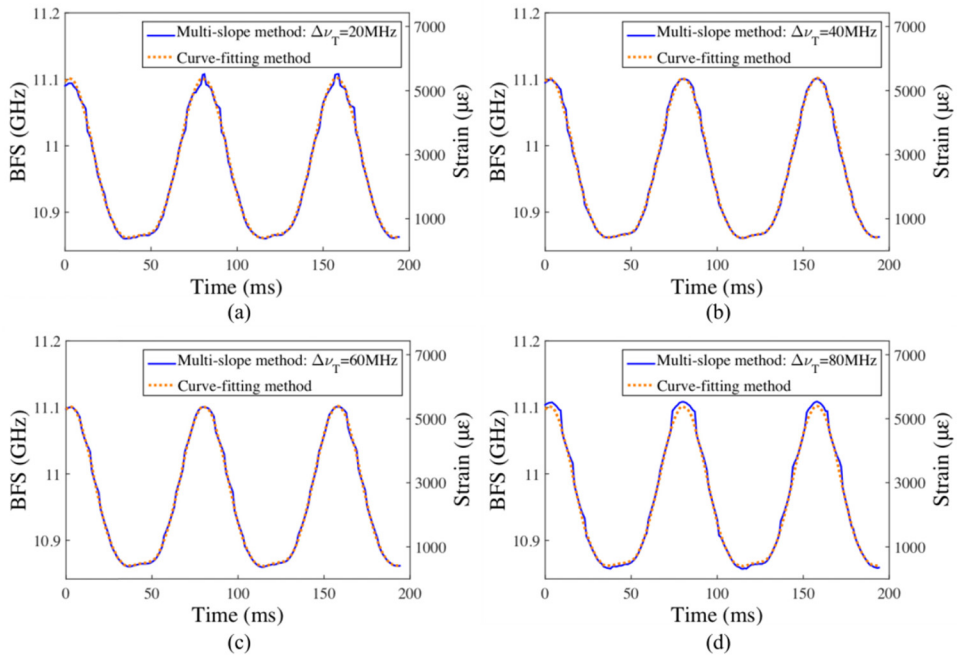

Fig. 8. Experimental results for the strain variation up to 5000με with a frequency of 12.8Hz: the solid curve shows the measured BFS via multi-slope assisted F-BOTDA and the dotted curve shows the results obtained via curve-fitting based F-BOTDA with a step of 4MHz.

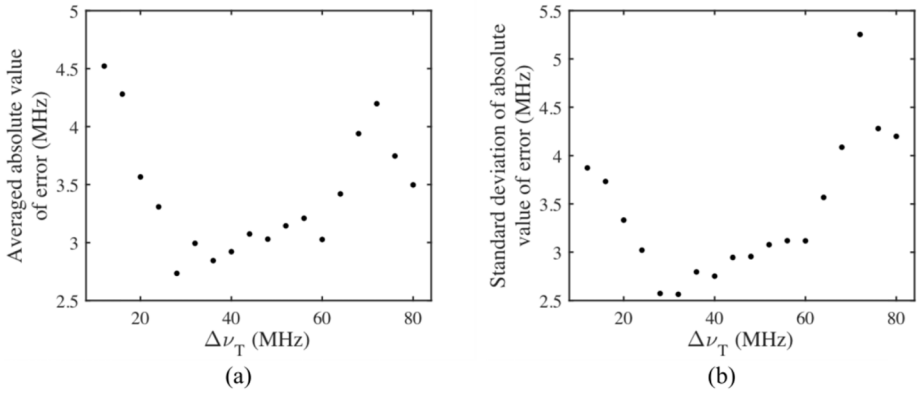

Fig. 9. Measurement error of BFS as a function of $\Delta\upsilon_T$

One frame of the measured BFS along the whole FUT is shown in Fig. 10, which is corresponding to Time = 2ms in Fig. 8 when the fiber is stretched to the maximum strain. This figure shows that a 2.3-m fiber is stretched for a 32-m fiber. In the stretched segment, the strain is not uniform because the friction between the FUT and the off-axis loads additional force on the segment of fiber.

#258384 Received 2 Feb 2016; revised 22 Apr 2016; accepted 23 Apr 2016; published 27 Apr 2016

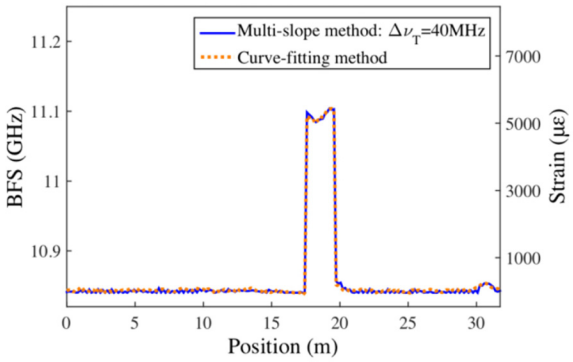

Fig. 10. Measured BFS along the FUT.

Another experiment is carried out to verify the feasibility of measuring irregular changed strains. A non-sine changed strain is loaded on the FUT and the measured BFS is shown in Fig. 11. The subfigure (a) is the measured BFS in time domain, where the blue curve shows the data obtained via multi-slope method when $\Delta\upsilon_T$ = 40MHz and υ_{PPm_0} = 10840MHz. Its power spectrum is shown in Fig. 11(b), which is achieved via fast Fourier transform. The measurement error of the BFS is shown in Fig. 12, which also implies that we can get a better measurement performance when $\Delta\upsilon_T$ equals about a half of the FWHM of the BGS.

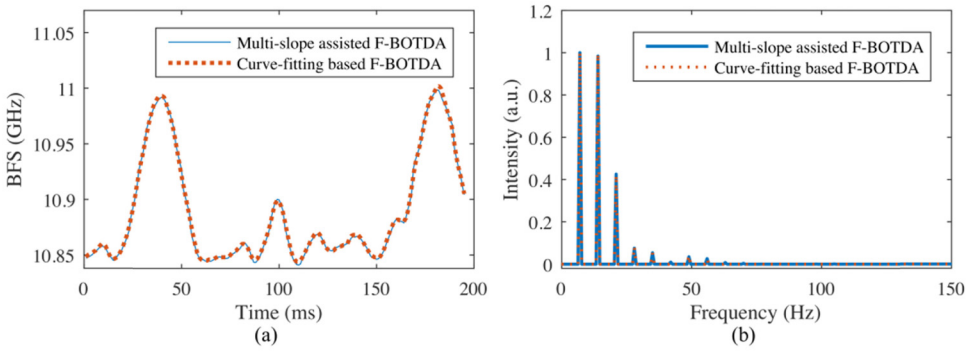

Fig. 11. Experimental results for the non-sine changed BFS: (a) the track of BFS in time domain and (b) its power spectrum. $\Delta\upsilon_T$ = 40MHz.

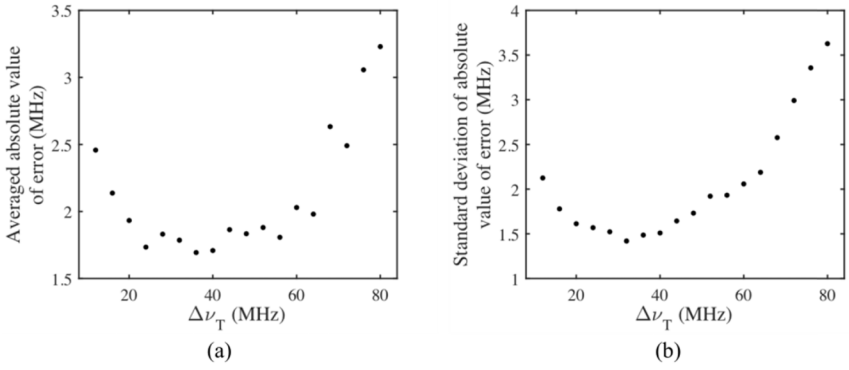

Fig. 12. Measurement error of BFS as a function of $\Delta\upsilon_T$ for non-sine changed strain.

#258384 Received 2 Feb 2016; revised 22 Apr 2016; accepted 23 Apr 2016; published 27 Apr 2016

The maximum frequency that can be measured by the multi-slope assisted F-BOTDA relies on several parameters, including the length of the FUT, the average times and the number of frequency components of probe tones that is determined by the maximum variation of BFS. According to the Nyquist sampling theorem, the maximum frequency of strain variation is described as:

$$f_{\max} = \frac{c}{4nL\left(\frac{\Delta\upsilon_{\mathrm{B\_max}}}{\Delta\upsilon_{\mathrm{T}}}+1\right)N_{avg}}. \tag{6}$$

Where L is the length of the FUT and $\Delta\upsilon_{\mathrm{B\_max}}$ is the maximum variation of the BFS. N_{avg} is the average times. Generally, $\Delta\upsilon_{\mathrm{T}}$ is much larger than the scanning step in the curve-fitting method, which results in that the sampling rate could be increased in a great amount in the multi-slope method, and finally leads to the improvement in high frequency dynamic strain sensing. Taking $\Delta\upsilon_{\mathrm{T}}$ = 40MHz for example, the maximum frequency that the multi-slope method can measure is up to 10 times as high as that of the curve-fitting method with the scanning step of 4MHz. The most significant reduction of time derives from the non-curve fitting algorithm for the demodulation of the BFS. According to our experiment, the time consumption of data processing could be reduced to less than one twentieth using the same calculation environment compared with the curve-fitting method.

For distributed dynamic strain measurements based on fast BOTDA, the measurement range is usually relative short (less than 1km in most cases) for achieving a high sampling rate. Although the price of PM fiber is higher than SMF, it allows a simple scheme and thus a reduced cost compared with standard SMF, which needs an additional setup to eliminate polarization fading. Considering both the short measurement range and simple scheme, a PM fiber is still preferable for the distributed dynamic strain measurement. For longer distance measurement, when SMF is used as FUT, the polarization fading should be overcome. One of the most often used method is to scramble the state of polarization (SOP), where an average over multiple data should be carried out [18]. As a result, the sampling rate is reduced significantly. Another choice is to employ a fast polarization switch. It can overcome the problem with the cost of reducing the sampling rate by half. Further, a double-orthogonal-pump method proposed by Moshe Tur's group may be a good choice, in which the sampling rate is not reduced with the cost of additional EOMs [23].

4. Summary

A dynamic distributed sensing technique based on multi-slope assisted fast BOTDA is proposed, which employs both double-slope demodulation and frequency-agile technique based on arbitrary waveform modulation. By using the frequency-agile technique, a probe sequence with several tones is constructed, which realizes an extension of the strain-measurement scale in a great amount. In experiment, the dynamic strain is measured via both multi-slope assisted F-BOTDA and curve-fitting based F-BOTDA. The latter is used to verify the feasibility of the multi-slope method and analyze its measurement precision. A sine-changed sensing of 5000-με strain with the frequency of 12.8Hz is measured, the spatial resolution of which is ~1m. Further, a non-sine changed strain is measured to test its ability of measuring irregularly varied strain. The measurement accuracy is analyzed theoretically and experimentally. The analysis shows that a measurement error of less than 3MHz could be obtained when the frequency difference of two adjacent probe tones equals approximately half of the width of the BGS.

The time consumption for data processing is a severe problem for real-time dynamic sensing, which could be much more than the time used for data acquisition in curve-fitting based F-BOTDA. The multi-slope method solves the problem by employing an algorithm

#258384 Received 2 Feb 2016; revised 22 Apr 2016; accepted 23 Apr 2016; published 27 Apr 2016

without curve-fitting to demodulate BFS, which considerably reduces the data processing time. Further, fewer tones are employed to detect the BFS compared with the curve-fitting method, which makes it possible to increase the maximum sampling rate up to 10 times. The maximum frequency that can be measured is up to tens of kHz in a 32-m PM fiber. Obviously, the faster measurement is achieved using less data and results in a compromise of accuracy. The multi-slope assisted F-BOTDA is a good candidate for real-time online monitoring system rather than a precise measuring. Further work aims to improve the measurement precision, especially for the suppression of the influence of width change of BGS.

Acknowledgments

Thanks to Prof. Avi Zadok, who gave me valuable suggestions on this paper. This work is supported by the 863 Program of China 2014AA110401, the National Key Scientific Instrument and Equipment Development Project 2013YQ040815, the NSF of China 61575052 and 61308004, the National Key Technology Research and Development Program of the Ministry of Science and Technology of China 2014BAG05B07, the Foundation for Talents Returning from Overseas of Harbin 2013RFLXJ013, the Scientific Research Fund of Heilongjiang Provincial Education Department 12531093, the Fundamental Research Funds for the Central Universities HIT. NSRIF. 2015041, the National Key Laboratory Funds for National Key Laboratory of Science and Technology on Tunable Laser and the Heilongjiang Postdoctoral Fund LBH-Z15076.

#258384 Received 2 Feb 2016; revised 22 Apr 2016; accepted 23 Apr 2016; published 27 Apr 2016